J|A|C|S ARTICLES

Published on Web 04/13/2010

Ab Inito Modeling of Ethylbenzene Dehydrogenase Reaction Mechanism

Maciej Szaleniec,*,† Tomasz Borowski,† Karola Schühle,‡ Malgorzata Witko,† and Johann Heider‡

Institute of Catalysis and Surface Chemistry, Polish Academy of Sciences, Niezapominajek 8, 30-239 Krakow, Poland, and Laboratory of Microbial Biochemistry, Philipps-University of Marburg, Marburg, Germany

Received August 26, 2009; E-mail: ncszalen@cyf-kr.edu.pl

Abstract: Density functional theory calculations were performed to study the mechanism of ethylbenzene oxidation by ethylbenzene dehydrogenase (EBDH). EBDH is a bacterial molybdopterin enzyme capable of stereospecific anaerobic hydroxylation of alkylaromatic compounds to secondary alcohols. It is a key biocatalyst in the metabolism of ethylbenzene-degrading bacteria such as *Aromatoleum aromaticum*, which converts ethylbenzene to (*S*)-1-phenylethanol. The recently determined EBDH structure enabled the theoretical description of the ethylbenzene oxidation mechanism. In this work, theoretical calculations and kinetic isotopic experiments were conducted and combined in order to elucidate the reaction mechanism. We considered three aspects: (i) Does the reaction concur with one two-electron or two one-electron transfers? (ii) Is the active site His192 important for the reaction and what is its protonation state? (iii) What catalytic consequences have different possible arrangements of the molybdopterin ligand? The most important outcome of the calculations is that mechanisms involving two one-electron transfers and a radical-type intermediate have lower energy barriers than the corresponding two-electron transfer mechanisms and are, therefore, more plausible. The mechanism involves two transition states: radical-type **TS1** associated with the C−H bond cleavage, and carbocation-type **TS2** associated with the transfer of the second electron and OH rebound. Using models with protonated and nonprotonated His 192, we conclude that this amino acid takes part in the mechanism. However, as both models yielded plausible reaction pathways, its protonation state cannot be easily predicted. Qualitative agreement was reached between the calculated kinetic isotope effects (KIE) obtained for radical **TS1** and the KIE measured experimentally at optimum pH, but we observed a very strong pH dependence of KIE throughout the investigated pH range (3.1 for pH 6, 5.9 for pH 7, up to 10.5 at pH 8.). This may be explained by assuming a gradual shift of the rate-determining step from **TS1** associated with high KIE to **TS2** associated with low KIE with lowered pH and an increasing contribution of proton/deuteron tunneling associated with high pH. Finally, models were calculated with different signs of the conformational twist of the pterin ligands, yielding only slightly different energy profiles of the reaction pathways.

Introduction

Ethylbenzene dehydrogenase (EBDH) is a molybdoenzyme belonging to the dimethyl sulfoxide (DMSO) reductase family, catalyzing the oxygen-independent, stereospecific hydroxylation of ethylbenzene to (*S*)-1-phenylethanol. It is the first known enzyme capable of direct anaerobic hydroxylation of a nonactivated hydrocarbon,[1,2] and is a key enzyme in the mineralization of ethylbenzene by *Aromatoleum aromaticum*, a denitrifying bacterium related to the genera *Azoarcus* and *Thauera*.

Recently, it was shown that EBDH oxidizes a range of aromatic or heterocyclic compounds with ethyl or propyl substituents[3] to secondary alcohols. The reaction is catalyzed by the enzyme using a molybdenum cofactor (MoCo), which in the native state consists of a molybdenum(VI) nucleus ligated by two molybdopterin guanine dinucleotide (MGD) ligands and an aspartic acid residue. Two electrons acquired by the cofactor during the reaction, i.e., the hydroxylation of the hydrocarbon, are then transferred via a chain of iron−sulfur clusters connecting the molybdenum with a heme b cofactor in the γ subunit, from which the electrons are donated to a yet-unknown acceptor. Notably, EBDH exhibits in vitro activity only with artificial electron acceptors of high redox potential, such as the ferricenium ion ($E^{0'} = +380$ mV). This suggests that its natural electron acceptor may be a periplasmic cytochrome *c* of similarly high potential, which would couple the ethylbenzene oxidation to the nitrate respiration of *A. aromaticum*. The fact that the free energy corresponding to the large redox potential difference, between the electron acceptor and the 1-phenyle-

† Institute of Catalysis and Surface Chemistry, Polish Academy of Sciences.

‡ Laboratory of Microbial Biochemistry, Philipps-University of Marburg.

(1) Kniemeyer, O.; Heider, J. *J. Biol. Chem.* **2001**, *276*, 21381–21386.
(2) Johnson, H. A.; Pelletier, D. A.; Spormann, A. M. *J. Bacteriol.* **2001**, *183*, 4536–4542.
(3) Szaleniec, M.; Hagel, C.; Menke, M.; Nowak, P.; Witko, M.; Heider, J. *Biochemistry* **2007**, *46*, 7637–7646.

 10.1021/ja907208k

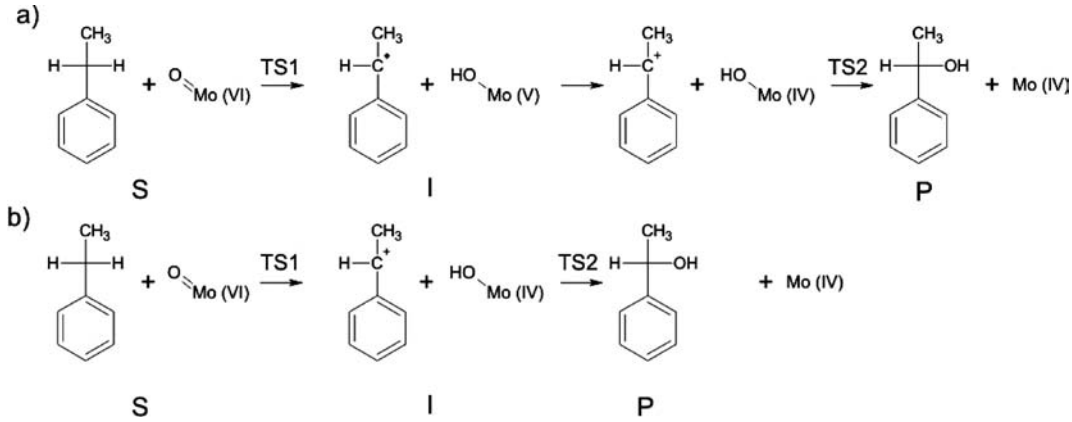

Figure 1. Reaction scheme of ethylbenzene oxidation by EBDH: (a) reaction pathway involving two one-electron steps: homolytic C−H activation leading to radical intermediate and an electron transfer coupled to OH-rebound: [**TS2**] indicates that these steps cannot be regarded separately (see text for further details); (b) reaction pathway involving heterolytic C−H activation, i.e., formally, a hydride transfer, leading to a carbocation intermediate.

thanol/ethylbenzene couple with an E^0 of +30 mV, is dissipated, explains the observed irreversibility of the reaction.[4]

Although enzymes containing MoCo are generally known to catalyze oxygen transfer reactions,[5] the established mechanisms of these enzymes are not compatible with hydroxylation reactions of hydrocarbons, which normally require activation through homolytic C−H cleavage. Therefore, the elucidation of the catalytic mechanism of EBDH is not only important for understanding the enzyme's chemistry, but it also makes a very interesting case study of MoCo-associated biochemistry.

Previous attempts to explain the reaction mechanism of EBDH have been based on experimental kinetic results and quantitative structure activity relationship (QSAR) studies.[3] These studies suggested a hypothetical reaction mechanism in which the C−H bond cleavage, supposed to be a rate-limiting process, leads to a carbocation intermediate. Such conclusions were reached by analyzing the influence of electronic (resonance and inductive) stabilization effects, introduced by various substituents of the aromatic ring, on the reaction kinetics. QSAR models used Hammett σ^+ parameters, which indicate the accumulation of positive charge in the rate-limiting transition state. However, a recent analysis of reaction kinetics, based on density functional theory (DFT)-derived descriptors such as changes of Gibbs free energies for carbocation or radical formation ($\Delta G^{\text{carbocation}}$ and $\Delta G^{\text{radical}}$), suggests that the actual mechanism might be more complicated.[6]

In general, C−H activation by EBDH may proceed either via homolytic (Figure 1a) or via heterolytic (Figure 1b) bond cleavage,[1,2,6] requiring either a radical-type transition state, or a more conventional two-electron reduction step of the MoCo without the formation of a substrate-derived radical, but rather a carbocation. In the step following the C−H bond cleavage, the OH group is rebound to the activated substrate species. Therefore, rate-limiting barriers can either be associated with C−H breaking (**TS1**) or with the OH rebound process (**TS2**). Finally, the oxidative half-cycle of the reaction is followed by a series of electron transfers toward the external electron acceptor and subsequent reoxidation of the enzyme molybdenum center. As QSAR kinetic experiments did not provide information on the type of rate-limiting step, a full and detailed description of the reaction mechanism must be complemented by theoretical modeling.

Therefore, detailed quantum chemical studies by DFT were performed on the mechanism of the oxidative part of the catalytic reaction. DFT has already been applied to elucidate the reaction mechanisms in molybdoenzymes such as DMSO reductase,[7] nitrate reductase (NAP),[8] and trimethylamine *N*-oxide reductase,[9] as well as for several model compounds.[10−14] These studies revealed that MoCo is involved in relatively straightforward reduction or oxidation reactions, where an oxygen atom is either transferred from an oxygen-rich substrate (e.g., DMSO, NO_3^-, $ONMe_3$) to the reduced molybdopterin (Mo^{IV}) or from Mo═O to an oxygen-deficient substrate, such as sulfite, formate, or triphenylphosphine.[8,11,15,16] In the case of ethylbenzene oxidation by EBDH, such a simple oxygen transfer reaction is not likely to be sufficient and must be complemented by some kind of activation of the hydrocarbon. The closest resemblance among other modeled MoCo enzymes may be the mechanism of xanthine oxidase,[17] where a C−H bond must initially be activated by a ligand of the cofactor, and then an OH group is transferred from MoCo to the activated substrate. However, xanthine oxidase belongs to a different class of molybdoproteins, with significant structural differences.

The reaction of EBDH starts with the oxidized form of the cofactor, while an X-ray structure is only known for the reduced enzyme. Therefore, a reliable prediction of the structure and energy of the oxidized form of the active site had to be set up as a prerequisite for the accurate modeling (**big model**).

(4) Kloer, D. P.; Hagel, C.; Heider, J.; Schulz, G. E. *Structure* **2006**, *14*, 1377–1388.
(5) Hille, R. *Chem. Rev* **1996**, *96*, 2757–2816.
(6) Szaleniec, M.; Witko, M.; Heider, J. *J. Mol. Catal. A: Chem.* **2008**, *286*, 128–136.
(7) McNamara, J. P.; Hillier, I. H.; Bhachu, T. S.; Garner, C. D. *Dalton Trans.* **2005**, 3572–3579.
(8) Leopoldini, M.; Russo, N.; Toscano, M.; Dulak, M.; Wesolowski, T. A. *Chem.—Eur. J.* **2006**, *12*, 2532–2541.
(9) Thapper, A.; Deeth, R. J.; Nordlander, E. *Inorg. Chem.* **2002**, *41*, 6695–6702.
(10) Thapper, A.; Deeth, R. J.; Nordlander, E. *Inorg. Chem.* **1999**, *38*, 1015–1018.
(11) Pietsch, M. A.; Hall, M. B. *Inorg. Chem.* **1996**, *35*, 1273–1278.
(12) Bray, M. R.; Deeth, R. J. *Inorg. Chem.* **1996**, *35*, 5720–5724.
(13) Ilich, P.; Hille, R. *Phys. Chem. B* **1999**, *103*, 5406–5412.
(14) McNaughton, R. L.; Lim, B. S.; Knottenbelt, S. Z.; Holm, R. H.; Kirk, M. L *J. Am. Chem. Soc.* **2008**, *130*, 4628–4636.
(15) Hernandez-Marin, E.; Ziegler, T *Inorg. Chem.* **2009**, *48*, 1323–1333.
(16) Voityuk, A. A.; Albert, K.; Romão, M. J.; Huber, R.; Rösch, N. *Inorg. Chem.* **1998**, *37*, 176–180.
(17) Hille, R. *Arch. Biochem. Biophys.* **2005**, *433*, 107–116.

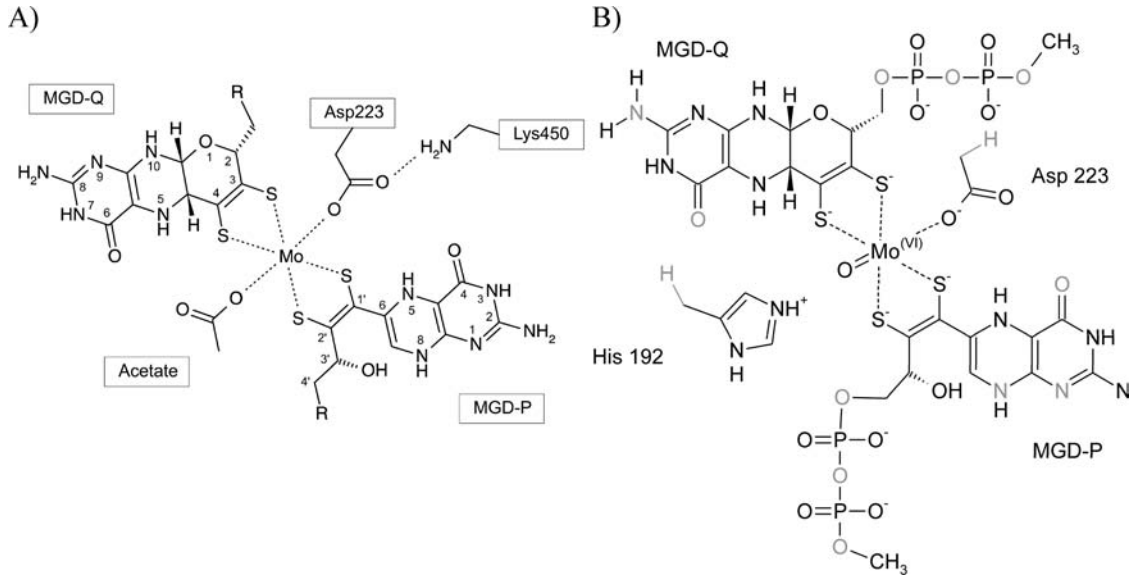

Figure 2. Schematic representation of the molybdenum active center in (A) the reduced EBDH, where R = (P_2O_7)-ribose-guanine nucleotide,[4] (B) the **big model** representing oxidized EBDH. The positions of the atoms in gray were constrained.

The EBDH active center contains a His[192] residue that is postulated to be involved in a proton shuttle network associated with ethylbenzene oxidation, and was included in the model. To assess the effects of different protonation of His[192], both states were used in the modeling. The models were validated by comparison with the experimentally measured KIE.

Moreover, the molybdenum cofactor in DMSO-reductase type enzymes appears to change its conformation profoundly between the reduced and oxidized state. In particular, the dihedral angle of the two dithiolene ligands of the Mo atom ($S_1-S_2-S_3-S_4$) is close to 0 in the reduced state, but its absolute value increases in the oxidized state. Principally, this can result in positive or negative values of the dihedral angle, which would result in two possible conformers of the oxidized enzyme. Because EBDH is one of few enzymes with nonidentical molybdopterin ligands (one containing an open and the other a closed pyran ring), we also addressed this possible conformational isomerism in calculating the reaction pathways.

Materials and Methods

Model Preparation. Big Model. The initial geometry of the reduced molybdenum cofactor was obtained from the recently published EBDH structure[4] (Figure 2A). To obtain a model for the oxidized enzyme, an oxo group was added as a ligand to the Mo, replacing an acetate ligand originating from the buffer in the original structure. The His[192] lying near the MoCo was suggested to be involved in a reaction mechanism[4] and therefore included in the cluster model.

The initial optimization was conducted with Gaussian 03[18] for a large model of the active center, where the main chain atoms of amino acids and guanine groups of nucleotides are replaced by methyls (see Figure 2B). The optimization led to a nearly octahedral arrangement of the six molybdenum ligands, similar to those found in previous models of other MoCo enzymes.[6−9] However, the optimized structure differs profoundly from that of the molybdenum cofactor in EBDH's closest related enzyme that is known in an oxidized form, i.e., nitrate reductase.[19,20] To obtain a more biologically relevant model of the EBDH active site, constraints were introduced in order to account for the influence of the protein. In the **big model,** the atoms with constrained positions are the following: pteridine ring atoms, which are able to form hydrogen bonds with nearby protein residues, CH groups in acetate and methylimidazole (Asp[223] and His[192] residues), as well as the bridging oxygen atoms in the diphosphate chains due to the multiple hydrogen bond contacts formed by these oxygens in the crystal structure (Figure 2B). Optimization with such constraints leads to a distorted trigonal prismatic coordination (Figure S1A of Supporting Information), an arrangement similar to that observed for the oxidized forms of other molybdoenzymes,[19,21−23] but with the $S_1-S_2-S_3-S_4$ dihedral angle of 30.5°, which is of the opposite sign to NarGH, the closest structural relative of EBDH. Therefore, another geometry optimization was conducted with the $S_1-S_2-S_3-S_4$ dihedral angle initially set to −20°, which yielded an angle of −43° in the optimized structure. Both possible conformers of MoCo are significantly different from the octahedral model complexes obtained without constraints (angles of ∼52° and −51°, respectively), but still deviate in the degree of the twist from the situation in nitrate reductase (dihedral angle −18.2° in NarGH). Other geometric features of the **big model** are in accordance with previously reported data for other molybdoenzymes (for more details see Supporting Information). Apparently, the protein matrix imposes more rigid constraints on the molybdenum cofactor than we were able to represent in our model. Nevertheless, the structures obtained constitute useful structural scaffolds for construction of smaller models, which are employed in investigating the reaction mechanism.

Small Models. Low pH Model 1. Based on the geometry obtained for the initial **big model,** a smaller model was constructed to study the actual reaction pathway. It contains the first coordination sphere of molybdenum, including the side chains of His[192] and Asp[223] and the pyran rings of the pteridine cofactors as present in EBDH (one cofactor in closed, one in open conformation).

(18) Frisch, M. J.; et al. *Gaussian 03*, Revision D.01; Gaussian, Inc.: Wallingford CT, 2004.
(19) Jormakka, M; Richardson, D.; Byrne, B.; Iwata, S. *Structure* **2004**, *12*, 95–104.
(20) Bertero, M. G.; Rothery, R. A.; Palak, M.; Hou, C.; Lim, D.; Blasco, F.; Weiner, J. H.; Strynadka, N. C. J *Nat. Struct. Biol.* **2003**, *10*, 681–687.
(21) Li, H.-K.; Temple, C.; Rajagopalan, K. V.; Schindelin, H. *J. Am. Chem. Soc.* **2000**, *122*, 7673–7680.
(22) Boyington, J. C.; Gladyshev, V. N.; Khangulov, S. V.; Stadtman, T. C.; Sun, P. D. *Science* **1997**, *275*, 1305–1308.
(23) Dias, J. M.; Than, M. E.; Humm, A.; Huber, R.; Bourenkov, G. P.; Bartunik, H. D. *Struct. Folding Des.* **1999**, *7*, 65–79.

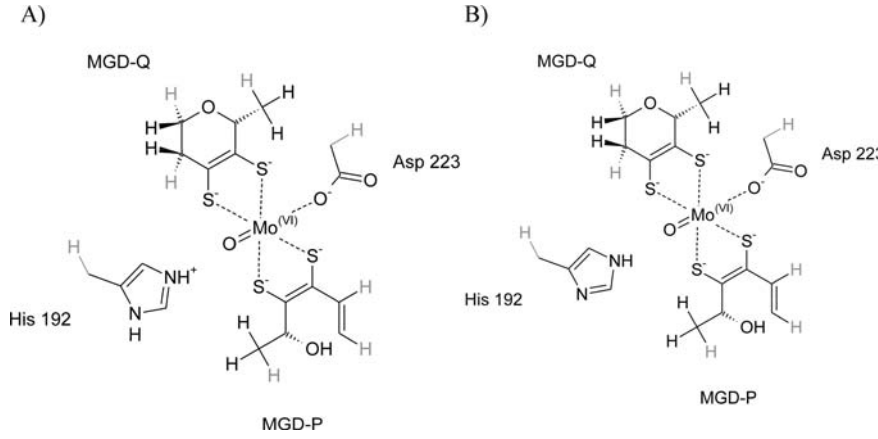

Figure 3. Schematic representation of small cluster models with constrained coordinates (A) 'low pH' **model 1** and (B) 'high pH' **model 2** (only one H atom on His[192]). Atoms with frozen coordinates are shown in gray.

Constraints were introduced by freezing the positions of hydrogen atoms introduced in place of cut bonds, as well as the Cβ carbon atoms of amino acid residues. It was verified that the model had enough conformational freedom to achieve a relaxed conformation in the reduced form, i.e., the structure obtained from the model agreed with that obtained by X-ray-crystallography (indicated e.g. by a $S_1-S_2-S_3-S_4$ dihedral angle close to 0°).

The position of ethylbenzene in the models used for mechanistic studies was retrieved from the structure of the EBDH−ethylbenzene complex, which was obtained from docking simulations. The docking of ethylbenzene was initiated with Autodock 3.0,[24] using a rigid model of the a-subunit, which had been modified by *in silico* replacement of the reduced cofactor with the model of the oxidized cofactor (**big model**).

The geometry of the **model 1** (Figure S2 and Table S3 of the Supporting Information) closely resembles that obtained with the **big model**, indicating that the reduction of the model size did not change the geometry of the active site significantly. A minor difference is that the hydrogen atom of the protonated His[192] is closer to the oxygen ligand of Mo compared to the **big model,** which is probably caused by the more pronounced charge effects of His[192] in the smaller model. As a result, the Mo═O bond is elongated (Figure S2, Supporting Information). Moreover, as the geometrical constraints in the smaller model are imposed closer to the molybdenum atom than in the case of the **big model**, the final $S_1-S_2-S_3-S_4$ dihedral angles are slightly different (33.5° and −37.6°) from the case of the **big model**.

High pH Model 2. The 'high pH' **model 2** is derived from **model 1** by deprotonation of the imidazole Nd atom. Because of the presence of the charge-neutral His[192], **model 2** exhibits a shorter Mo═O bond length and a weaker H-bond between the oxo group and the Nε−H of His[192] than that found in **model 1** (Figure 3B and Table S3 of the Supporting Information). The deprotonation of the Nε atom with rotation of heteroaromatic ring was also considered but turned out to be less likely, since the geometric constraints prevent His[192] from developing optimal interactions with both the oxo ligand and the hydrocarbon.

Computational Procedures. The DFT calculations were performed using a spin-unrestricted B3LYP functional.[25] Geometry optimization and vibration calculations were conducted with the 6-31G(d,p) basis set for light atoms and the LANL2DZ effective core potential and basis set for Mo.

Only singlet reaction pathways were considered in the model, because in the previous studies on *Desulfovibrio desulfuricans* nitrate reductase (NAP),[8] a reaction pathway on the singlet potential energy surface was found to be energetically preferred over a mechanistically similar triplet pathway. This conclusion was also confirmed in our preliminary studies.[26]

For mechanisms involving homolytic cleavage, we started with the optimization of the intermediate product (**I**) in the triplet state, followed by conversion to a singlet state. This allowed for the breaking of the $\alpha-\beta$ orbital symmetry, which was necessary to describe the mechanism correctly. For the mechanisms involving heterolytic cleavage, orbital symmetry did not have to be broken. Therefore, the former calculations resulted in open shell systems, and the latter in closed shell systems. The transition states were localized by potential energy scans along the reaction coordinates followed by full optimization of TS geometries using the Berny algorithm. Single-point energies were calculated with the lacv3p** basis, both in the gas phase and in solvent (assuming a polarized continuum model with $\varepsilon = 4$), and all Mulliken charges discussed were obtained from single-point calculations in the model solvent. The obtained electronic energies were corrected by including zero-point energies obtained from B3LYP/6-31 g(d,p) frequency calculations and employing a scaling factor of 0.98. The Stable[27] check was performed for each single-point energy calculation and showed that there are no lower-energy states for the obtained geometries of stationary points. To calculate kinetic isotopic effects, the thermal energy corrections, obtained at the B3LYP/6-31 g(d,p) level, were calculated for the temperature of the experimental enzyme assays (35 °C). The influence of the tunneling effect was assessed with the Wigner tunneling correction[28] where imaginary frequencies were scaled with the factor 0.9620.

Enzyme Assays - Kinetic Measurements. EBDH for enzymatic assays was purified as described previously.[4] The activity of EBDH was measured as the decrease of absorption of ferricenium tetrafluoroborate at 290 nm.[1,3,4] Reactions were started by addition of 1 mM ethylbenzene or ($^2H_{10}$)ethylbenzene, respectively. The pH optima of the reactions were determined using 50 mM MES/KOH buffer in the range of pH 4.5−7.5 or 50 mM HEPES/KOH buffer in the range of pH 6.0−9.0.

Results

The reaction of EBDH starts with the oxidized (Mo^{VI}) enzyme, whereas only the structure of the reduced enzyme (in the Mo^{IV} state) is available. Therefore, the modeling of the reaction mechanism required an initial model of the enzyme in

(24) Morris, G. M.; Goodsell, D. S.; Halliday, R. S.; Huey, R.; Hart, W. E.; Belew, R. K.; Olson, A. J. *J. Comput. Chem.* **1998**, *19*, 1639–1662.
(25) Becke, A. D. *J. Chem. Phys.* **1993**, *98*, 5648–5652.
(26) Szaleniec, M.; Borowski, T.; Witko, M.; Heider, J. *The anaerobic oxidation of ethylbenzene by ethybenzene dehydrogenase - modeling of the mechanism*; TheoBio-07, Conference material of 3rd Symposium on Theoretical Biophysics, Cetraro (Cosenza), Italy, 2007.
(27) Bauernschmitt, R.; Ahlrichs, R. *J. Chem. Phys.* **1996**, *104*, 9047–9052.
(28) Wigner, E. P. *Z. Phys. Chem.* **1932**, *B19*, 203.

the oxidized form. We modeled the active center in several forms, starting with an essentially complete representation of the two molybdopterin cofactors and the coordinating amino acids, which was then simplified to enable the efficient DFT calculation of the reaction path.

Our modeling addressed three major questions concerning the mechanism in question: (i) does the sign of the relative twist of the molybdenum dithiolene ligands ($S_1-S_2-S_3-S_4$ dihedral angle between molybdopterins) influence chemistry and energetics of the overall catalytic process? (ii) Does the mechanism involve two subsequent electron transfers and a radical intermediate, or does it involve one 2-electrons oxidation step with the formation of a carbocation species? (iii) Is the reaction mechanism sensitive to the protonation of the His^{192} residue, and can the pH-dependent shift in the observed KIE be correlated with results of calculated KIE?

To answer the first question, all models were considered in two versions with positive or negative $S_1-S_2-S_3-S_4$ dihedral angles. To answer the second question, two different types of reaction pathways were considered, assuming either homolytic or heterolytic C−H cleavage. Finally, in order to address the third question, models with His^{192} in either protonation state were applied. In total, this leads to the construction of eight independent reaction pathways. To provide a clear picture of this quite complicated matter, we will describe the homolytic reaction pathways first, and then the heterolytic ones. Whenever possible, geometric and electronic data concerning both types of conformers are provided, and the issue of active-site conformation will be discussed separately.

Twist of Pterin Ligand. Because the initial optimization of the active-site model differed in the sign of dihedral angle of the dithiolenes from that of the closest known structural analogue, NarGH, we constructed a second model where a negative angle was enforced. Calculations were then conducted using both models (called positive and negative twist conformers in the following) to assess the contribution of the dithiolene conformation on the mechanism.

The main difference between negative and positive twist conformers is that the reaction energy barriers calculated for the negative twist conformer were lower than those obtained for the positive twist conformer. This is mostly because the **S** species exhibit slightly higher energies in the negative twist models (6−16 kJ mol^{-1}, see Table S6, Supporting Information) than in the corresponding positive twist models. If the absolute energy values obtained from the calculations are compared with the energy values of the **S** species of the positive twist conformers (the lowest **S** species energies), the relative energies of **TSs** turn out to be very similar for both conformers (see Table S6, Supporting Information). The general chemistry of the reaction mechanism (i.e., the electronic and geometrical characteristics of the transition states) calculated for the two possible conformers of molybdopterins turned out to be insensitive to the sign of the dithiolene twist. Also for both conformers, a gradual decrease was observed of the absolute values of $S_1-S_2-S_3-S_4$ dihedral angles when MoCo was reduced from Mo^{VI} via Mo^{V} to Mo^{IV} similarly to the results obtained by McNamara et al.[29]

Two One-Electron Transfers versus One Two-Electron Transfer. Radical Reaction Pathway 1 - Low pH Model 1. Modeling of a homolytic reaction mechanism (**pathway 1**) yielded the energetic profile shown in Figure 4A. The detailed energy values with zero-point energy corrections are given in Table S1 of the Supporting Information (see also Table S2, Supporting Information). The reaction can be divided into two parts: the first consists of C−H cleavage proceeding through **TS1** and generating a radical intermediate and one-electron reduced central metal (Mo^{V}), whereas the second part proceeds with the abstraction of a second electron from the radical intermediate and the rebound of a hydroxyl group to the hydrocarbon cation, which is associated with the reduction of the active-site molybdenum to Mo^{IV}. The energies given in the following section are calculated in PCM model solvent and refer to the conformers with positive values of the $S_1-S_2-S_3-S_4$ dihedral angle; those for the negatively valued conformers are given in brackets. Full data including energies calculated both in the gas-phase and PCM model solvent are shown in Table S1, Supporting Information.

The activation of ethylbenzene appears to be possible when the substrate molecule approaches the oxo ligand with its methylene group. As a result, the pro-S-hydrogen atom is transferred to the Mo═O group. In **TS1** the modeled structure of the substrate-derived species is close to that of an ethylbenzyl radical as indicated by an almost flat conformation around the radical carbon (alkyl-ring dihedral angle −162°), a shortened bond between C1 and the aromatic ring (from 1.52 Å to 1.46 Å), and a characteristic deformation of the benzene ring[6] (see Table S3 of the Supporting Information). Moreover, the calculated spin population of ethylbenzene is 0.56 (respectively 0.54 for the negative angle conformer). Subsequently, the intermediate species **I** is obtained by completing the transfer of both hydrogens from His^{192} and ethylbenzene to the Mo═O group, thereby forming a water ligand, which is stabilized by hydrogen bonds to His^{192} and Asp^{223}. Geometrically, **TS1** is closer to the intermediate species **I** than to the substrate form, with the $S_1-S_2-S_3-S_4$ dihedral angle of 12.9° (−29.5°) and 15.1° (−20.3°), respectively, and Mo−O···H distance smaller than the C···H distance (see Figure 5, Table S3 of the Supporting Information).

Modeling of the further steps of the reaction revealed that Mo^{V} is reduced to Mo^{IV} before **TS2** is reached, formally forming an ethylbenzyl carbocation, as indicated by the calculated spin and charge populations of the activated hydrocarbon (spin: 0.0 and charge: +0.6, for both conformers). **TS2** is characterized by an additional movement of the water ligand of Mo toward the ethylbenzyl carbocation, assisted by the hydrogen bonding of one proton to Ne of His^{192}. Finally, the product-bound species is formed by simultaneous transfer of the proton of the water ligand to His^{192} and the OH^- group to the ethylbenzene carbocation, forming (*S*)-1-phenylethanol. In the product-bound species, the reduced molybdenum center is five-coordinated, as seen in the crystal structure.[4] The bound alcohol is not released spontaneously in our model, because of the hydrogen bonds with His^{192} and Asp^{223}. Therefore, we assume that this process involves a significant activation barrier.

The differences of the energies are shown in panels A and E of Figure 4, revealing that the predicted barrier heights are in a reasonable range. The energies of **TS1** and **TS2** were calculated as 117.1 kJ mol^{-1} and 114.2 kJ mol^{-1}, respectively, for the positive twist model (96.8 kJ mol^{-1} and 99.2 kJ mol^{-1} for the negative twist model). Although it may be considered that the rate-limiting step is different for the two conformers (**TS2** for the positive and **TS1** for the negative twist model), the

(29) Webster, Ch. E.; Hall, M. B. *J. Am. Chem. Soc.* **2001**, *123*, 5820–5821.

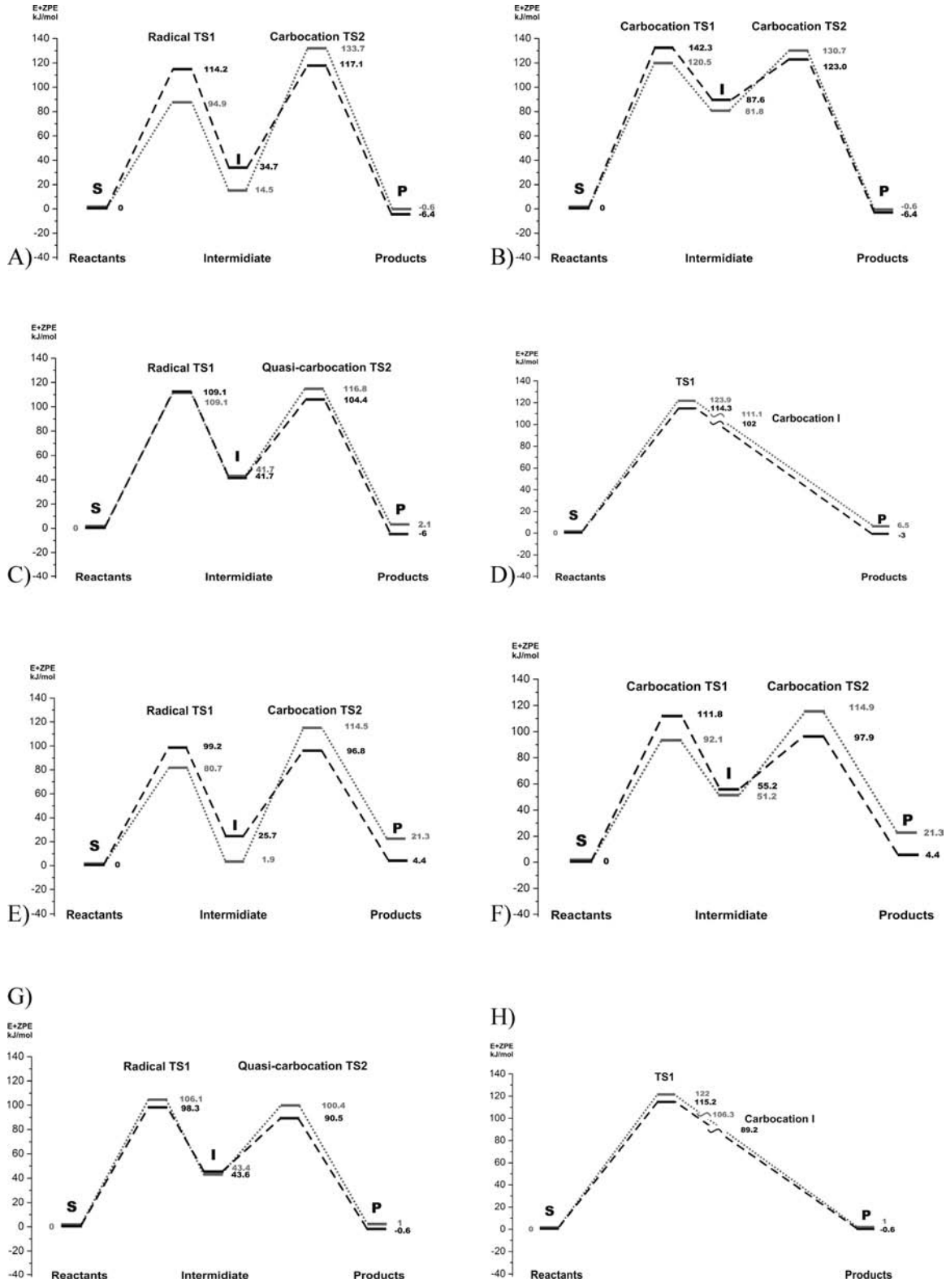

Figure 4. Energetic profiles along the reaction coordinate obtained: (i) with the positive twist conformer - low pH model: (A) homolytic **reaction pathway 1**; (B) heterolytic **reaction pathway 3**; high pH model: (C) homolytic **reaction pathway 2**; (D) heterolytic **reaction pathway 4**; and (ii) with the negative twist conformer - low pH model: (E) homolytic **reaction pathway 1;** (F) heterolytic **reaction pathway 3**; high pH model: (G) homolytic **reaction pathway 2**; (H) heterolytic **reaction pathway 4**. **S** oxidized enzyme−substrate complex, **TS1** (C−H) cleavage transition state, **I** intermediate product, **TS2** OH rebound transition state 2, **P** reduced enzyme−product complex. Gray dotted line: gas-phase calculations; black dashed line: PCM model solvent calculations. Numbers provide energy differences between **S** and particular stationary points in kJ mol^{-1}. Reference energies are the same for homolytic and heterolytic pathways.

energy values are, in fact, so close that it is not possible to determine the rate-limiting step.

Radical Reaction Pathway 2 - High pH Model 2. To assess the influence of different protonation states of His^{192} on the

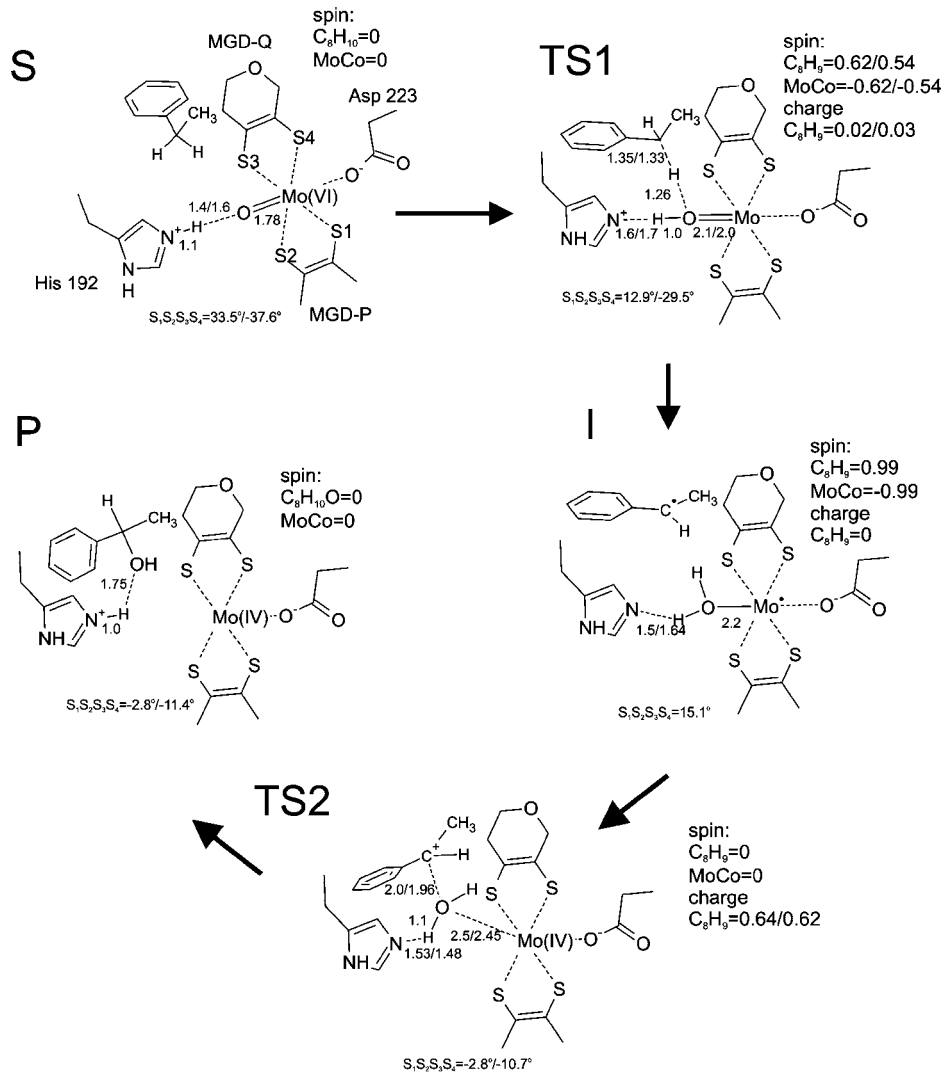

Figure 5. EBDH-catalyzed oxidation of ethylbenzene to S-1-phenylethanol for low pH **reaction pathway 1** (positive twist/negative twist conformers). **S** oxidized enzyme−substrate complex, **TS1** C−H cleavage transition state, **I** intermediate product, **TS2** OH rebound transition state 2, **P** reduced enzyme−product complex.

reaction, a model containing a deprotonated His[192] was constructed (see Figure 3B). Both protonation states, represented by the active-site models, may coexist over the enzyme's pH activity range, but the actual pH value, at which the shift between **pathways 1** and **2** occurs, i.e., His[192] deprotonates, is very hard to predict.

The proposed mechanism starts with ethylbenzene approaching the Mo═O group and the shift of the pro-S−H atom of C1 of ethylbenzene toward the oxo group to generate **TS1** in a homolytic manner similar to that suggested for **pathway 1**. During the transition to the **I** species, the pro-S−H atom is fully transferred to the oxo group, but no proton shift from the His[192] occurs. Therefore, a hydroxyl ligand is attached to the Mo in this model, rather than a water ligand. As in **pathway 1**, for **I** the active center contains Mo(V) and the activated hydrocarbon exhibits a clearly radical charge-neutral characteristics (hydrocarbon spin 1.0, and no charge). The **TS2** corresponds to a state just before the final electron transfer. At this point, the cofactor is almost in the reduced Mo^{IV} state with a hydroxyl ligand bridging to the quasi-carbocation intermediate of ethylbenzene (hydrocarbon spin population 0.12 with positive charge of 0.43/0.48). At a C−O distance just a fraction of an Å shorter than that observed in **TS2**, the system becomes spin-restricted, and a closed-shell carbocation is formed, as in the case of **reaction pathway 1**. Finally, (*S*)-1-phenylethanol is obtained by bond formation between the carbocation and the hydroxyl group.

The energy of **TS1** is 109.1 kJ mol^{-1} (98.3 kJ mol^{-1} for the negative twist conformer) and the energy of **TS2 is** 104.4 kJ mol^{-1} (90.5 kJ mol^{-1} for the negative twist conformer). In contrast to the situation found in the low pH model, the barriers for the first step, connected with **TS1,** are significantly higher, and thus **TS1** is considered the rate-limiting step for both twist conformers (see C and E of Figure 4).

Two Electron-Transfer Reaction Pathways. The proposed mechanisms for most molybdenum enzymes involve two-electron transfer reactions rather than one-electron transfers and associated radical intermediates. Therefore, a possible alternative mechanism of EBDH involving heterolytic C−H cleavage was evaluated by modeling the reaction with a closed shell approach, using **models 1** and **2** to represent the possible variations in His[192] protonation. Assuming the presence of a protonated His[192] (**reaction pathway 3**), the C−H bond cleavage involves a two-electron oxidation of ethylbenzene to a carbocation-type intermediate **I**, concomitant with a reduction of Mo^{VI} to Mo^{IV}. In **TS1**, the oxo ligand of Mo^{VI} is converted to a water ligand of Mo^{IV} with elongated O−H bonds, indicating the transfer of the

pro-S−hydrogen of C1 of ethylbenzene and the Nε−hydrogen from His[192]. The full reduction to a Mo^{IV} species is indicated by the change of the $S_1-S_2-S_3-S_4$ dihedral angle (Table S3 and Figure S3 of the Supporting Information) associated with transition from the **S** species to **TS1** (from 33.4° to 2.3° for the positive twist and from −37.6° to −6° for the negative twist model) with the final values characteristic for reduced MoCo structures.[4,29−31] The angle is then almost constant throughout the following reaction steps. However, the analysis of charges indicates that the carbocation is not yet formed in **TS1** (the charges of the hydrocarbon moiety are +0.32 and +0.2 for the positive and negative twist model, respectively). Transition to the **I** species does not result in profound changes in the geometry compared to **TS1**, except for the complete transfer of the pro-S−hydrogen to the Mo−water ligand and the completion of the two-electron transfer, as indicated by the increase in the charge of the activated hydrocarbon (+0.01 in **TS1** to +0.5 in **I** in the positive, and −0.1 in **TS1** to +0.4 in **I** in the negative twist model). The transition to **TS2** in this mechanism relates to the transfer of a hydroxyl group to the carbocation intermediate. **TS2** still contains ethylbenzene in the form of a carbocation (charge of carbocation +0.68/+0.62 for positive/negative twist models), whereas Mo remains in the reduced state (Mo^{IV}). The Mo-bound water is ready to dissociate to a proton, which reprotonates His[192], and the hydroxyl group that attacks the carbocation. This leads directly to formation of the product-bound state. The **TS1** energies are 142.3 kJ mol^{-1} (111.8 kJ mol^{-1} for the negative twist conformer), while the **TS2** energies are 123.0 kJ mol^{-1} (97.9 kJ mol^{-1} for the negative twist conformer), which predicts **TS1** as a rate-limiting step (see B and F of Figure 4).

In the presence of a deprotonated His[192] (**reaction pathway 4**), it was not possible to identify a transition state associated with OH rebound for either conformer, as the optimization of the **I** species led directly to the product complex **P**. Therefore, the barrier associated with **TS1** seems to be the only important one.

The geometry of **TS1** in **pathway 4** exhibits an $S_1-S_2-S_3-S_4$ dihedral angle (16.9°/−17.6°) and Mo−S bond lengths (average 2.44 Å) similar to the value characteristic for Mo(V) compounds (see Table S3 and Figure S4 of the Supporting Information). The charge of the activated hydrocarbon changes from −0.14 (−0.08) in **S** species to +0.02 (+0.05) in **TS1**. In contrast to **reaction pathway 3**, no carbocation is formed in **TS1**. However, when the C−H cleavage is completed, the charge of the activated carbocation becomes positive (+0.34/+0.3), while the geometry of the cofactor attains a $S_1-S_2-S_3-S_4$ dihedral angle characteristic for reduced MoCo (0.22°/−8.3°, see Table S3 of the Supporting Information). From this point the reaction proceeds to the product **P** without additional barriers. The energy barrier for such C−H cleavage is rather high, at 114.3 kJ mol^{-1} (115.2 kJ mol^{-1} for the negative twist conformer).

The difference between the energies of the rate-limiting steps of the low pH radical (**pathway 1**) and carbocation mechanisms (**pathway 3**) is significant (positive conformer: 25.2 kJ mol^{-1}, negative conformer: 12.6 kJ mol^{-1}). A very similar situation is found comparing the high pH radical (**pathway 2**) and carbocation mechanisms **(pathway 4)** (positive conformer: 5.2 kJ mol^{-1}, negative conformer: 16.9 kJ mol^{-1}). (Figures 4 D and 4H).

This indicates that homolytic C−H cleavage (**pathway 1** or **2**) is energetically more favorable than the corresponding heterolytic mechanisms (**pathway 3** or **4**).

Isotope Effect. In order to validate the results of the modeling, we decided to compare them with experimental results. To distinguish between possible variation of the reaction mechanism and determine **TS1** or **TS2** as the rate-limiting steps, the kinetic isotopic effects were calculated with ethylbenzene and ($^2H_{10}$)ethylbenzene and compared with experimental values from corresponding kinetic measurements.

The isotope effects were calculated for all transitions states in all reaction pathways. As the experimental kinetic measurements were conducted with ($^2H_{10}$)ethylbenzene at 35 °C (308 K), the same species was used to calculate energy thermal corrections. Therefore, the kinetic constants were calculated according to the eq 1.

$$k_X = \frac{k_B T}{h} e^{\left(-\frac{\Delta(E + \text{Thermcorr})_X}{RT}\right)} \quad (1)$$

where X stands for either H or D. The isotope effect was calculated as the ratio of k_H to k_D. Tables S3A and S3B (Supporting Information) collect all calculated energy barriers, rate constants, and KIE for all models.

In order to estimate whether tunneling effects may be involved in the observed kinetics, the obtained KIEs were corrected by Wigner's tunneling correction $\Gamma(T)$[28]. Although Wigner correction is very simple (eq 2), it is frequently reported to yield good consistency with experimental values.[32,33]

$$k(T) = \Gamma(T)\, e^{\left(-\frac{\Delta(E + \text{Thermcorr})_X}{RT}\right)}$$
$$\Gamma(T) = 1 + \frac{1}{24}\left(\frac{h|\nu^*|}{k_b T}\right) \quad (2)$$

Regardless of the type of the mechanism, a significant isotope effect associated with C−H cleavage (**TS1**) is calculated, which for homolytic mechanisms is in the range of 6.5−7.5 (see Tables S3A and S3B, Supporting Information). Transition states associated with OH/OH_2 group rebound (**TS2**) exhibit k_H/k_D with values close to 1. The k_H/k_D values calculated with Wigner's tunneling correction yield KIE values associated with C−H cleavage in the range of 9−10.6 and an almost negligible correction of KIE associated with the OH/OH_2 group rebound (1.0−1.3).

The experimental determination of KIE was done by measuring conversion rates with deuterated and nondeuterated ethylbenzene. Surprisingly, the enzyme assays yielded a quite different pH optima for the conversion of ($^2H_{10}$)ethylbenzene than that of ethylbenzene conversion (Figure 7A) (pH 6.5 and 7.5, respectively). As a result, we observed linearly increasing kinetic isotope effects (k_H/k_D) with the pH values almost spanning the entire range of enzyme activity (Figure 7B, Table S5, Supporting Information). The observed KIE values ranged from 3.1 at pH 6 to 10.5 at pH 8.5. Only at higher pH, k_H/k_D dropped to 7.3, most probably due to the inactivation of EBDH. The determined KIE of the enzyme under optimal conditions was 6.9. Therefore, we conclude that the reaction rate is limited by **TS1** and the mechanism probably follows **pathway 2** in high

(30) Donahue, J. P.; Goldsmith, Ch. R.; Nadiminti, U.; Holm, R. H. *J. Am. Chem. Soc.* **1998**, *120*, 12869–12881.
(31) Enemark, J. H.; Cooney, J. J. A.; Wang, J.-J.; Holm, R. H. *Chem. Rev.* **2004**, *104*, 1175–1200.

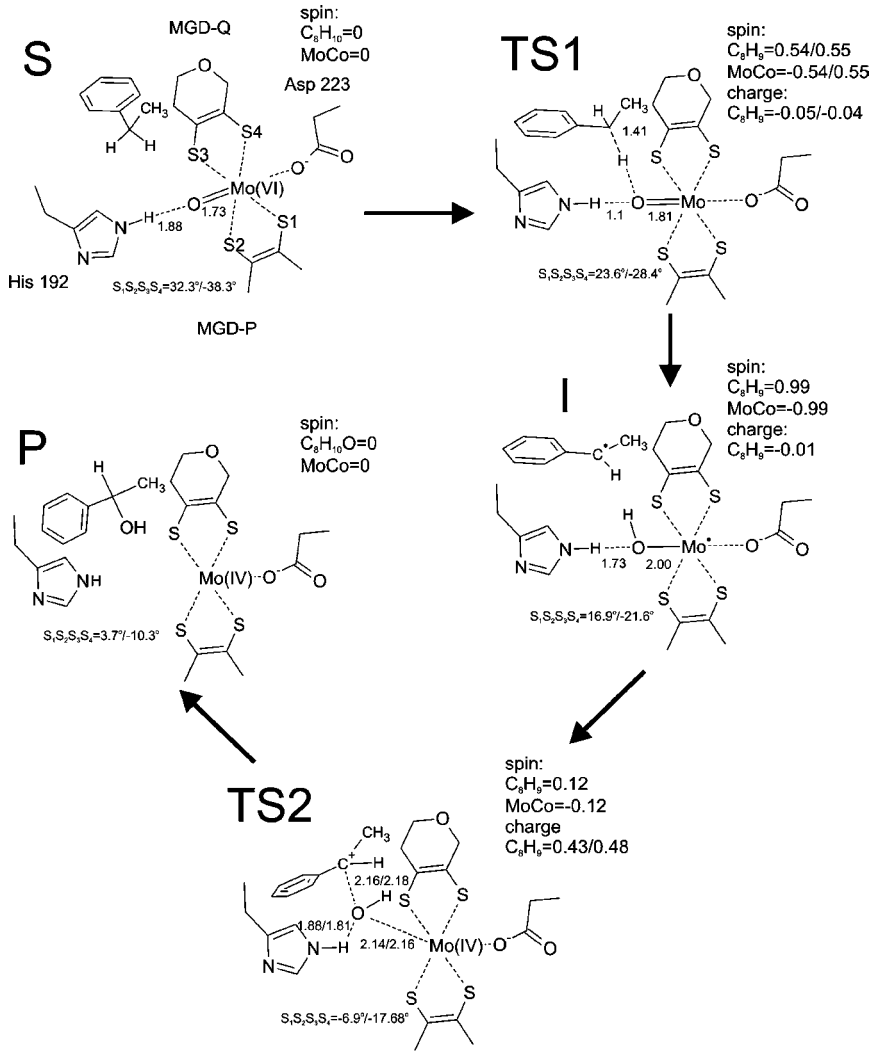

Figure 6. EBDH-catalyzed oxidation of ethylbenzene to S-1-phenylethanol for high pH **reaction pathway 2** (positive twist/negative twist conformers).

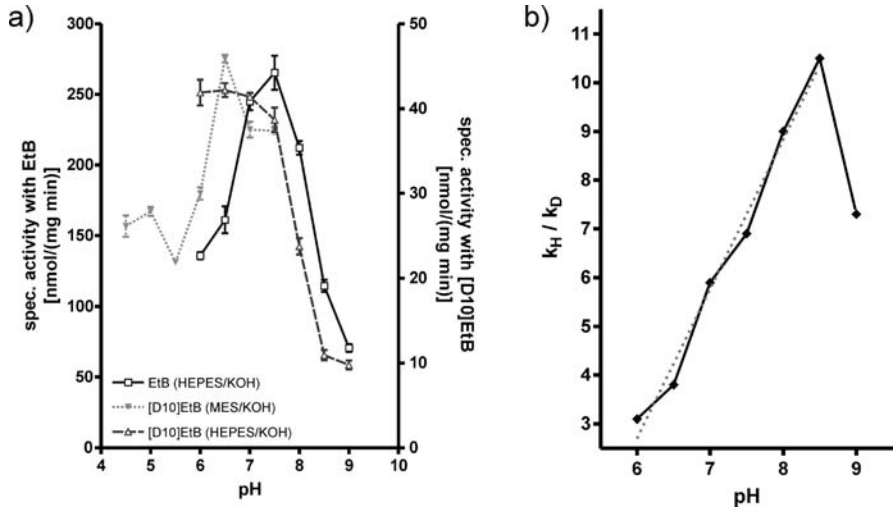

Figure 7. pH dependence of kinetic isotope effect. (a) pH dependence of EBDH activity with ethylbenzene (black line with squares; pH 6.0−9.0 as determined in HEPES/KOH buffer; right *Y* axis) and ($^2H_{10}$)ethylbenzene (gray dotted line; pH 4.5−7.5 as determined in MES/KOH buffer and dark gray dashed line; pH 6.0−9.0 as determined in HEPES/KOH buffer; right *Y* axis). (b) Kinetic isotope effect (k_H/k_D) is increasing with increasing pH. Dotted line: linear fit (pH 6−8.5, $R^2 = 0.9863$).

pH conditions, but it appears to shift to a less affected mechanism at lower pH values.

Discussion

The mechanism of ethylbenzene oxidation by *Aromatoleum aromaticum* ethylbenzene dehydrogenase has been investigated by means of quantum-mechanical methods. Based on the results, several conclusions can be drawn.

On the basis of the coordinates of the reduced cofactor extracted from the EBDH crystal structure, the geometry of the oxidized MoCo was predicted by means of gas-phase QM optimization. The optimized structure suggests that the cofactor is kept in the entatic state, which significantly facilitates the catalytic process. The gas phase geometry optimization of cluster models led to S_1-S_2-S_3-S_4 dihedral angle around 30° in the **S** state and 15° in the **I** state for a positive twist conformer and approximately −40° and −19°, respectively, in the **S** and **I** states for a negative twist conformer.

The reaction pathways involving homolytic C−H cleavage turned out to be energetically more favorable than those associated with hydride transfer. As a result, the EBDH mechanism involves two energy barriers: **TS1**, associated with radical type C−H cleavage, and **TS2,** associated with carbocation formation and OH group rebound. Therefore, the hypothesis presented previously[3,5,4] seems to be confirmed. The next question to be answered was whether **TS1** or **TS2** would be the rate-limiting step of the reaction. The calculated mechanisms indicate that under high pH conditions, **TS1** seems to be rate-limiting regardless of the model, whereas under low pH conditions, the energy values of **TS1** and **TS2** were very close and the predicted rate-limiting steps of the two twist models did not agree. Therefore, we propose that the rate-limiting step of the reaction may actually change from **TS1** under high pH conditions to **TS2** under low pH conditions. This assumption would also explain the observed pH dependence of the KIE, which drops from 6.9 at optimum pH to 3.1 at pH 6. From the calculated gas-phase energies of the low pH models (Table S1, Supporting Information), one might suspect that the applied solvent correction might be overcompensated, because the gas-phase energy values clearly suggest **TS2** as the rate-limiting step.

However, for higher pH values even higher isotopic effects are observed than calculated based on the classical transition-state theory for C−H cleavage. The observed values (up to KIE 10.5) can be easily explained if proton tunneling is taken into account. We have employed only a simple Wigner correction,[28] but it yielded very good agreement with the observed value for the high pH model (Wigner corrected KIE equals 10.2/10.75). In our opinion this result suggests that, under high pH conditions, the tunneling effect is more pronounced, yielding a higher value of KIE.

The proposed catalytic role of His^{192} 4 was further supported for either of the two possible protonation states. The protonated His^{192} residue donates a H^+ to the OH ligand of Mo in **TS1,** forming a water ligand in the **I** state, which is in turn shuttled back to the carbocation of ethylbenzene. In the deprotonated state, His^{192} forms a hydrogen bond with the oxo or hydroxyl ligand of Mo, but proton shift and water formation do not occur. The His^{192} proton shuttle seems to stabilize the radical **I** species, as the energies observed for **pathway 1** are lower by approximately 27/42 kJ mol^{-1} (∼7/18 kJ mol^{-1} in PCM for positive/negative twist) than those for **pathway 2**. The protonation state of His^{192} influences the electronic nature of **TS2**. For protonated reaction **pathway 1** the second electron is transferred from the radical hydrocarbon onto the molybdenum center before the **TS2** is reached. This results with carbocation species present in the transition state. Meanwhile, for the high pH model the electron transfer is not yet finished when the **TS2** state is reached, leaving a quasi-carbocation species with both positive charge and fractional spin density.

For any six-coordinated Mo^{VI} complexes, an octahedral geometry is the most energetically favorable. For Mo^{V} complexes, the optimal coordination is trigonal antiprismatic, and for five-coordinated Mo^{IV} complexes the optimal coordination is tetragonal pyramidal.[24,25] According to the crystal structures of NarGH[19] and other oxidized enzymes of the DMSO reductase family, the oxidized cofactor is usually in a distorted trigonal antiprismatic conformation, rather than an octahedral one.[22,23] This strained conformation of the active site is enforced by the enzyme scaffold and lowers the energetic barrier of the reaction, according to the entatic principle.[34] This hypothesis is also supported for EBDH by the energy difference observed between the optimized structures with and without geometrical constraints that were calculated for **model 1** (data not shown). The energy difference evaluated for the Mo^{VI} **S** species in **model 1** equaled 52 kJ mol^{-1} in PCM (51.4 kJ mol^{-1} for negative twist conformer) and 64 kJ mol^{-1} in gas phase (60 kJ mol^{-1} for negative twist conformer), which suggests a significant increase in the energy of the substrate-bound **S** species in the enzyme compared to the octahedral complex. A much smaller geometry relaxation between constrained and nonconstrained models is observed for the Mo^{V} complexes (**I** species) and almost none for the Mo^{IV} complexes (**P** species).

Similar results were obtained in modeling the reaction catalyzed by DMSO reductase. In works of Webster and Hall[29] constriction of the sulfur atom positions in the geometry of the transition state led to a significant elevation of the energy of the oxidized Mo^{VI} model by 37 kJ mol^{-1} and only a small elevation of that of the reduced Mo^{IV} model by ∼4 kJ mol^{-1}. This was interpreted as indication for the important role of strain imposed on the cofactor by the protein ligands, leading to a decreased exothermicity of the DMSO reduction. In terms of ethylbenzene oxidation by EBDH, a similar effect would reduce endothermicity of the reaction (resulting in an overall energetic difference close to 0) and decrease the height of the energy barrier. In a more recent work of McNaughton et al.,[14] the effect from the strain was estimated to be as large as 96 kJ mol^{-1}. In this case, the protein introduces a twist to the reduced cofactor. The authors argue that the resulting destabilization of the DMSOR **S** species decreases the activation energy and provides substrate access to the redox orbital. In our calculations on the EBDH model system, we predict a much more constrained geometry in the **S** species than in the **I** species, indicating that the catalytically active cofactor (i.e., oxidized Mo^{VI}) is similarly activated by distortion of its preferred ligand coordination.

In addition, the energies of the EBDH reaction pathways were calculated and compared for the positive and negative twist conformers, resulting in slightly higher energy values of the **S** species in the negative twist conformers. Although this effect might be only a model-artifact, it could also be associated with

(32) Gonzalez, C.; McDoual, J. J. W.; Schlegel, H. B. *J Phys Chem.* **1990**, *94*, 7467–7471.
(33) Tzima, T. D.; Papayannis, D. K.; Melissas, V. S. *Chem. Phys.* **2005**, *312*, 169–176.
(34) Williams, R. J. P. *Eur. J. Biochem.* **1995**, *234*, 363–381.

the elevation of the substrate energy and help in overcoming the reaction energy barriers in the actual enzyme.

All these studies suggest that the respective enzyme is primed for the reaction by imposing strain on the Mo-cofactor that supports the conversion of either reduced cofactor into the oxidized form or vice versa according to the entatic principle. Therefore, working with cofactor models that take into account the constraints posed by the respective enzyme appears to be crucial for the accurate description of the reaction mechanism and correct estimation of activation energy. Ideally, this can be achieved by QM:MM optimization of the complete enzymatic system followed by investigation of the C−H cleavage reaction within such a big system.

Conclusions

The mechanism of ethylbenzene oxidation by EBDH has been investigated by quantum chemical methods. Combined theoretical and experimental studies point toward radical C−H cleavage as the initial reaction and rate limiting step. A possible alternative hydride transfer seems to be less likely. The mechanism concludes with conversion of the hydrocarbon to a carbocation intermediate and rebound of a hydroxide to form the hydroxylated product. A histidine residue (His^{192}) of the active site is apparently involved in the reaction mechanism. The evaluation of different protonation states of His^{192} and their contribution to kinetic isotope effects indicates that it is most probably in the nonprotonated state under optimal pH conditions. However, an unusual linear dependence of KIE values with different pH values has been observed experimentally, which may indicate a shift of the reaction mechanism with varied pH values and some involvement of proton tunneling during C−H cleavage. The geometry of the cofactor and strain introduced by the protein appears crucial for the evaluation of activation energy. The cofactor ligation in the enzyme seems to introduce strain into the oxidized cofactor in order to facilitate the MoCo reduction and oxidation of the substrate.

Acknowledgment. We acknowledge the computational Grant KBN/SGI2800/PAN/037/2003, Grant N301 093036, and the financial support of the project 'Biotransformations for pharmaceutical and cosmetics industry' No. POIG.01.03.01-00-158/09-00 part-financed by the European Union within the European Regional Development Fund.

Supporting Information Available: Relative energies of investigated pathways with ZPE and solvent corrections (Table S1), raw energies of investigated pathways (Table S2A for positive twist and Table S2B for negative twist conformers), geometrical features of the investigated models (Table S3 A/B for positive/negative conformers), results of kinetic isotopic effect calculations (Table S4), results of kinetic isotopic effect measurements (Table S5), comparison of positive and negative twist energies (Table S6). Three-dimensional and schematic figures of **big models** (Figure S1) and low pH **S** species models (Figure S2) for both investigated conformers as well as geometries of reaction **pathways 3** and **4** (Figure S3 and S4). Full reference 18. Cartesian coordinates for each of the stationary points of the reaction pathways. As **S** and **P** species for the heterolytic pathways are identical to those of the respective homolytic ones, they were not repeated. This material is available free of charge via the Internet at http://pubs.acs.org.

JA907208K